60, 1091 (1977); (d) E. Baggiolini, H. P. Hamlow, and K. Schaffner, *J. Am. Chem. Soc.*, **92**, 4906 (1976); (e) G. W. Shaffer and M. Pesaro, *J. Org. Chem.*, **39**, 2489 (1974).

(9) Earlier studies on the stereochemistry of the methane carbon for the oxadi-π-methane reaction include: (a) S. Domb, G. Bozzato, J. A. Saboz, and K. Schaffner, *Helv. Chim. Acta*, **52**, 2436 (1969), and S. Domb and K. Schaffner, *ibid.*, **53**, 677 (1970), for δ-oxo-α,β-unsaturated keto; (b) T. Matsura and K. Ogura, *J. Am. Chem. Soc.*, **89**, 3850 (1967), and D. A. Plank and J. C. Floyd, *Tetrahedron Lett.*, 4811 (1971), for δ-ketocyclopentenones; (c) J. I. Seeman and H. Ziffer, *Tetrahedron Lett.*, 4413 (1973), a ${}_{\pi}2_s + {}_{\sigma}2_s$ analogue; (d) H. Sato, K. Nakanishi, J. Hayashi, and Y. Nakadaira, *Tetrahedron*, **29**, 775 (1973).

(10) Recent reports on the stereochemistry of the oxadi-π-methane reaction in addition to ref 1 include: (a) B. Winter and K. Schaffner, *J. Am. Chem. Soc.*, **98**, 2022 (1976); (b) W. G. Dauben, G. Lodder, and J. D. Robbins, *ibid.*, **98**, 3030 (1976); and (c) W. G. Dauben, G. Lodder, and J. D. Robbins, *Nouv. J. Chim.*, **1**, 244 (1977).

(11) (a) P. Crabbé, "ORD and CD in Chemistry and Biochemistry", Academic Press, New York, 1972, pp 40–42; (b) E. Bunnenburg, C. Djerassi, K. Mislow, and A. Moscowitz, *J. Am. Chem. Soc.*, **84**, 2823, 5003 (1962); (c) see also, T. Akiyama, D. Redder, J. U. Silverton, J. I. Seeman, and H. Ziffer, *J. Org. Chem.*, **40**, 3675 (1975).

(12) Only the forward reaction was examined under these experimental conditions. A thorough study would require irradiation of **4a** also.

(13) In addition to the product structures considered here, structure i is also possible. However, spectral data (kindly provided by Professor Peter Wharton, Wesleyan University) showed that our photoproduct was *not* i.

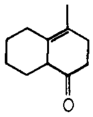

i

(14) J. J. Plattner and H. Rapaport, *J. Am. Chem. Soc.*, **93**, 1758 (1971).

(15) (a) A structurally similar photoequilibrium was reported by J. R. Williams and G. M. Sarkisian, *Chem. Commun.*, 1564 (1971). See also ref 9c. (b) This difference was also pointed out in our earlier communication (ref 1a, footnote 13). (c) N. C. Yang and R. H.-K. Chen, *J. Am. Chem. Soc.*, **93**, 530 (1971).

(16) This consideration has appeared previously in various forms in discussions of the [1,3] and type I photochemistry of β,γ-unsaturated ketones.[4c,7b–d,17] None of these studies has examined the structural features in detail, however (see ref 4c, p 62).

(17) (a) J. Gloor, K. Schaffner, and O. Jeger, *Helv. Chim. Acta*, **54**, 1864 (1971); (b) K. G. Hancock and R. O. Grider, *J. Am. Chem. Soc.*, **96**, 1158 (1974).

(18) (a) R. C. Lamb, P. W. Ayers, and M. K. Toncy, *J. Am. Chem. Soc.*, **85**, 3483 (1963); (b) C. Walling and A. Cioffari, *ibid.*, **94**, 6059, 6064 (1972); (c) M. Julia, *Pure Appl. Chem.*, **40**, 553 (1974).

(19) (a) The lifetimes of β,γ-unsaturated ketone singlets cluster around 1–5 ns,[19b] which is sufficiently long to allow conformational equilibrations to occur. (b) See, for example, J. C. Dalton, M. Shen, and J. J. Snyder, *J. Am. Chem. Soc.*, **98**, 5023 (1976), and D. I. Schuster, J. Eriksen, P. S. Engel, and M. A. Schexnayder, *ibid.*, **98**, 5025 (1976).

(20) (a) C. V. Neywick, Ph.D. Thesis, University of Kansas, 1974. (b) J. H.-S. Liu, unpublished results. (c) M. J. Mirbach, A. Henne, and K. Schaffner, *J. Am. Chem. Soc.*, **100**, 7127 (1978).

(21) We thank Professor M. D. Harmony for his advice and use of his instrument in this attempted structural analysis.

(22) A preliminary report of the synthetic aspects of this reaction has appeared: R. G. Carlson, R. L. Coffin, W. W. Cox, and R. S. Givens, *Chem. Commun.*, 501 (1973).

(23) Triplet-sensitized [1,3] migrations have been observed in other β,γ-unsaturated ketones: see (a) M. A. Schexnayder and P. S. Engel, *Tetrahedron Lett.*, 1153 (1975), and P. S. Engel and M. A. Schexnayder, *J. Am. Chem. Soc.*, **97**, 145 (1975). (b) R. S. Givens and W. K. Chae, *ibid.*, **100**, 6278 (1978).

(24) After these studies on the stereochemistry of the "methane" carbon were communicated, several variations and subsets of the originally proposed mechanistic triad[6] have appeared. Two of the most popular are given in Chart I.

(25) H. E. Zimmerman, T. P. Gannett, and G. E. Keck, *J. Am. Chem. Soc.*, **100**, 323 (1978).

(26) I. M. Tegmo-Larsson, H.-Y. Gonzenbach, and K. Schaffner, *J. Am. Chem. Soc.*, **59**, 1376 (1976). Recent CIDNP studies do suggest that there is a temperature dependence for the [1,3] acyl migration reaction. K. Schaffner, private communication.

(27) This point has been appreciated by some[4b,c,10b,c] though not by all.[4d,10a] The cyclopentenylcyclopentanone system, on examination of molecular models as well as our attempted microwave structure analysis, appears to be free of the structural constraints imposed on other alicyclic β,γ-unsaturated ketones.

(28) (a) See ref 4, 9, and 10, and references therein. (b) D. I. Schuster, R. H. Brown, and B. M. Resnick, *J. Am. Chem. Soc.*, **100**, 4504 (1978); D. I. Schuster and B. M. Resnick, *ibid.*, **96**, 6223 (1974); D. I. Schuster and R. H. Brown, *J. Chem. Soc., Chem. Commun.*, 28 (1976). (c) J. S. Swenton, R. M. Blankenship, and R. Sanitra, *J. Am. Chem. Soc.*, **97**, 4941 (1975). (d) P. S. Mariano and J.-K. Ko, *ibid.*, **94**, 1766 (1972).

(29) D. Varach, C. Quannes, and J. Hacques, *Bull. Soc. Chim. Fr.*, 1662 (1965).

(30) H. O. House and H. W. Thompson, *J. Org. Chem.*, **26**, 3729 (1961).

(31) C. G. Hatchard and C. A. Parker, *Proc. R. Soc., Ser. A*, **235**, 598 (1956).

(32) F. Arnot, "Organic Syntheses", Collect. Vol. II, Wiley, New York, 1943, p 165.

Reactions of Photoradicals with Nitroxide Spin Labels[1]

James R. Sheats[2] and Harden M. McConnell*

*Contribution from the Stauffer Laboratory for Physical Chemistry,
Stanford University, Stanford, California 94305.*

Received December 6, 1978

Abstract: The kinetics of reactions of radicals R· with nitroxide spin labels have been studied, the radicals R· being produced by laser photodecomposition of alkylcobalt complexes having the general formula $Co(CN)_5{}^{3-}R$. The rate of reaction of the radicals R· and nitroxide radicals is shown to be a sensitive function of the molecular environment of the nitroxide group, i.e., whether it is bound to a membrane or is free in solution. The ease with which a variety of alkylcobalt compounds $Co(CN)_5{}^{3-}R$ can be prepared with the corresponding radicals R· having different physical and chemical properties, and the ease with which the rate of generation of radicals R· can be varied with laser power, indicates that a number of applications of this photochemistry to biophysical and biochemical problems may be possible.

Introduction

In a recent communication Sheats and McConnell[3] reported the photochemical reaction of an alkylcobalt complex, carboxymethylpentacyanocobaltate, with the nitroxide 4-hydroxytetramethylpiperidine-1-oxyl (Tempol, or R_2NO) according to the equation

$$Co(CN)_5{}^{3-}\text{-}CH_2CO_2{}^- + R_2NO \xrightarrow{h\nu} Co(CN)_5{}^{3-} + (R_2)NOCH_2CO_2{}^- \quad (1)$$

Since then a number of applications to the study of phospholipid membranes have appeared[4,5] which illustrate the considerable scope and versatility of this class of reactions in biophysical chemistry. Although our interest in these reactions has been primarily in applications based on the stoichiometry of radical-radical reactions, we have recently found that a quantitative analysis of the kinetics of these reactions may also yield significant biophysical information. Here we report our results on two different alkylcobalt complexes, and describe preliminary applications to the structure and dynamics of model membranes (lipid bilayers).

0002-7863/79/1501-3272$01.00/0

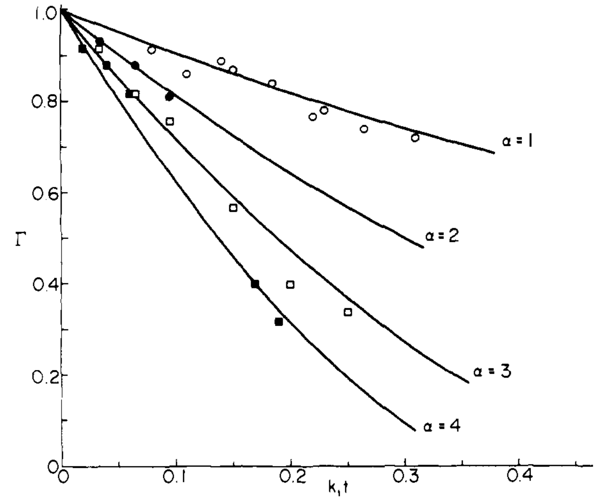

Figure 1. Relative EPR signal intensity Γ vs. the product of k_1 and time for the photolysis of Tempol and $Co(CN)_5{}^{3-}$-$CH_2CO_2{}^-$. Initial concentration of $Co(CN)_5{}^{3-}$-$CH_2CO_2{}^-$ was 1.0×10^{-3} M; initial concentrations of Tempol were such that (see text) (○) $\alpha = 1$; (●) $\alpha = 2$; (□) $\alpha = 3$; (■) $\alpha = 4$. The solid lines are calculated from eq 6 with $\beta = 10$; k_1 is obtained from initial rate data as described in the text. Laser power density was 34 mW/cm^2 (65 mW total beam power), $T = 24$ °C. Uncertainties are ±1.5 s, ±0.03 relative concentration unit (Γ), and ±10% in absolute concentrations.

Experimental Section

Materials. The preparation and characterization of the alkylcobalt complexes have been described previously.[3,5] We gratefully acknowledge the gift of (*N*-methyl)pyridylbromomethane from M. A. Schwartz.[5] Tempol was prepared by standard procedures.[6] Phospholipids were obtained from either Calbiochem or Sigma and a purity of ≥99% established by thin layer chromatography of the lipid and gas chromatography of fatty acid methyl esters.

Preparation of Samples. Solutions were deoxygenated by flushing several times with argon. (Loss of water during this procedure was <1%.) Reaction mixtures were placed via syringe in preflushed 50-μL pipets, which serve as EPR sample tubes; the pipets were sealed either by a septum cap or permanently with a torch. The carboxymethyl complex is not noticeably sensitive to room light; however, the pyridylmethyl complex decomposes fairly rapidly in room light when mixed with nitroxide (first half-life of about 30 min), so all operations with it were conducted under red light. (It was verified that green light does not cause decomposition; the reaction is due entirely to blue and near-UV wavelengths.)

The preparation of phospholipid membrane samples was carried out as described in ref 4.

Kinetic Experiments. Samples were exposed to the beam of a Spectra-Physics 164-05 argon ion laser, 3511- and 3543-Å lines, TEM_{00} mode, expanded 20 × by a pair of lenses. Total beam power was typically 50–250 mW (measured by the built-in power meter). The 50-μL capillaries, filled to a height of 10 mm, were placed perpendicularly in the center of the beam. (The variation in intensity of the Gaussian beam over the length of the sample was thus about 10%.) EPR spectra were recorded on a Varian E-4. Optical absorption spectra were recorded on a Cary 15. The wavelength dependence of the reaction of the carboxymethyl complex was determined using a mercury arc source and monochromator (Bausch and Lomb), provided by Professor B. S. Hudson.

The procedure for photolyzing phospholipid multilayer samples was exactly the same as that described in ref 4, except that no mask was used in the present work.

All bulk solution experiments were carried out at room temperature (20–24 °C), without thermostating. (Heating of the samples by the laser beam can be shown to be completely negligible for these conditions.[7]) The multilayer experiments were thermostated with a circulating water bath (Forma Scientific). The reactions were started and stopped by moving a barrier in and out of the beam path by hand, and times recorded with a stopwatch. The uncertainty in time by this procedure is about ±1.5 s.

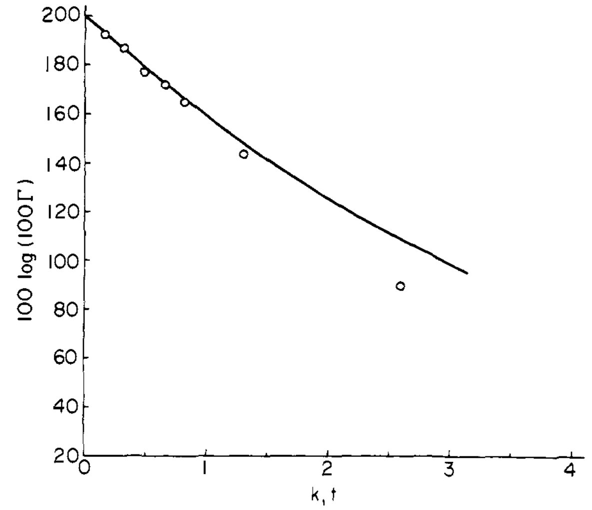

Figure 2. Logarithm of relative EPR signal intensity (measured as 100 log (100Γ); see text) vs. the product of k_1 and time for the photolysis of Tempol and $Co(CN)_5{}^{3-}$-$CH_2CO_2{}^-$, initially 5.0×10^{-3} M each. The line is calculated from eq 6 with $\beta = 10$. Photolysis with mercury arc source, $\lambda = 367$ nm, power density 26 mW/cm^2, $T = 24$ °C. Here $k_1 = 5.4 \times 10^{-3}$ s^{-1}; when adjusted for light intensity and extinction coefficient ($\epsilon_{353}/\epsilon_{367} = 1.26$), this agrees with the value in Table I.

EPR signal intensities were taken directly from first derivative peak-to-peak heights. For bulk solution experiments the uncertainty (due mainly to positioning of samples in the resonance cavity and the incomplete uniformity of illumination of the tube length) is about ±3%. For multilayer experiments the positioning error was less but a small amount of line broadening by the $Co^{II}(CN)_5{}^{3-}$, which could only be estimated, caused the uncertainty to be about ±8%, and somewhat greater at the end of the reaction where the spectrometer signal-to-noise became less favorable.

Results

Experimental Observations. The following features of the reaction of $Co(CN)_5{}^{3-}$-$CH_2CO_2{}^-$ and

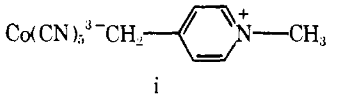

i

with Tempol in homogeneous solution were established.

(1) The initial rate of disappearance of nitroxide (hereafter referred to simply as "the initial rate") is linear in alkylcobalt concentration and independent of nitroxide concentration, at least for concentrations in the range 10^{-2}–10^{-4} M (Figure 1).

(2) The course of the reaction out to near completion is shown for various cases in Figures 1–3, where it is qualitatively apparent that neither first- nor second-order kinetics is being obeyed. Figure 2 shows an apparent first-order decay for the carboxymethyl complex with the ratio of initial concentrations of alkylcobalt to nitroxide (which we call α) equal to 1, but in Figure 1 it is seen that, with $\alpha = 3$ or 4, an essentially linear decay is seen out to very long times. The pyridylmethyl complex (Figure 3) shows an apparently exponential decay for 2 half-lives (though not beyond) with $\alpha = 2.2$, but closely approximates second-order decay with $\alpha = 1.4$.

(3) The initial rate varies linearly with incident power at constant wavelength, and linearly with extinction coefficient of the alkylcobalt complex for varying wavelength at constant power; thus the quantum yield of the photochemical event is independent of wavelength. (This behavior has been reported by Endicott and co-workers[8-10] for related reactions.) The lack of any dependence on the extinction coefficient of the nitroxide argues against participation by the excited state of the nitroxide. Photolysis of the nitroxide alone leads to no reaction

Table I. Parameters for Photolysis of Alkylcobalt Complexes with Tempol[a]

	k_1	P	ϕ	β	ϵ_{350}
$Co(CN)_5{}^{3-}CH_2CO_2{}^-$	0.010	34	0.16	10	265
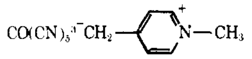	0.040	78	0.016	2	1.1×10^4

[a] Rate constants k_1, incident power density P (in mW/cm^2), quantum yield ϕ, $\beta = k_2/k_{-1}$, and molar extinction coefficients ϵ at 350 nm, for photolysis of alkylcobalt complexes at 350 nm, 22 °C, in aqueous solution (see text). k_1 is calculated using eq 7 and the data of Figures 1 and 3; estimated uncertainty ± 20%. β is obtained from eq 6 and the same data; estimated uncertainty ±30%. ϕ is calculated by the equation $\phi = k_1/2.303P\epsilon$ (ln 10). P is obtained by dividing the total beam power in a circle of radius 1 cm by the area of the circle.

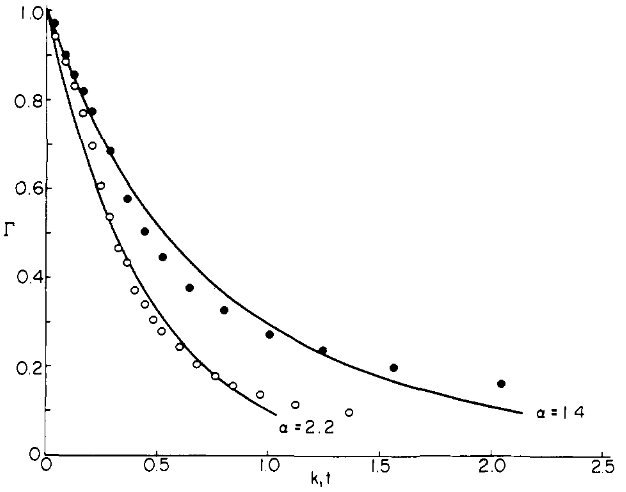

Figure 3. Relative EPR signal intensity Γ vs. the product of k_1 and time for the photolysis of Tempol and $Co(CN)_5{}^{3-}$ (*N*-methyl)pyridylmethyl. $\alpha = 1.4$: $A_0 = 1.3 \times 10^{-4}$ M. $\alpha = 2.2$: $A_0 = 1.0 \times 10^{-4}$ M. Solid lines are calculated with $\beta = 2$. Laser power 150 mW (78 mW/cm^2), $T = 24$ °C.

whatever, even after very long times and at very high power (300 mW; 10^{-4} einsteins/cm^2·s).

(4) As long as the incident light intensity is not raised orders of magnitude higher than $\sim 10^{-7}$ einsteins/cm^2·s, the stoichiometry is exactly as given in eq 1, and no other organic products were seen by gas chromatography-mass spectrographic analysis. Thus, significant dimerization of alkyl radicals does not occur under our conditions.

(5) The initial rate obtained from nitroxide EPR signal intensity was the same as that obtained from optical absorption spectra for the pyridylmethyl complex. For the most part the EPR method was preferable for several reasons: (a) with the carboxymethyl complex, with its much lower extinction coefficient, there is significant interference from nitroxide and $Co(CN)_5OH$ bands; (b) the EPR allows a wider range of concentrations to be sampled more easily; (c) later work with phospholipid membrane samples can only be done with EPR.

Kinetic Scheme. The kinetic scheme which accounts for these observations and which is in accord with expectations based on previous work in alkylcobalt photochemistry is as follows.

$$\underset{(C)}{Co(CN)_5{}^{3-}R} \underset{k_{-1}}{\overset{k_1}{\rightleftarrows}} \underset{(D)}{Co(CN)_5{}^{3-}} + \underset{(B)}{R\cdot} \tag{2a}$$

$$\underset{(A)}{(R_2)NO} + \underset{(B)}{R\cdot} \xrightarrow{k_2} (R_2)NOR \tag{2b}$$

The absence of alkyl radical dimerization, along with the results of alkylcobalamin flash photolysis studies,[8] indicates applicability of the steady-state assumption to the alkyl radical concentration; hence the rate equations are (using the notation defined in eq 2)

$$\frac{dA}{dt} = \frac{-k_1k_2AC}{k_2A + k_{-1}D} \tag{3a}$$

$$\frac{dC}{dt} = -k_1C\left[1 - \frac{1}{k_2A/k_{-1}D + 1}\right] \tag{3b}$$

and the steady-state alkyl radical concentration is

$$B = \frac{k_1C}{k_2A + k_{-1}D} \tag{4}$$

If the conditions $B \ll A$, $B \ll C$ are valid, then we can write $A = A_0 - (C_0 - C)$, $C = A - A_0 + C_0$, and $D = C_0 - C = A_0 - A$, where subscript 0 indicates initial concentration. With the definitions $\Gamma = A/A_0$, $\alpha = C_0/A_0$, and $\beta = k_2/k_{-1}$ the rate equation becomes

$$\frac{d\Gamma}{dt} = \frac{-k_1\beta(\Gamma - 1 + \alpha)}{(\beta + 1/\Gamma - 1)} \tag{5}$$

and the integrated form is

$$k_1t = \left(-\frac{1}{\beta}\right)\left\{\left(\frac{1}{\alpha - 1}\right)\ln\Gamma + \left[\left(\frac{1}{1 - \alpha}\right) - 1 + \beta\right] \times \ln\left[\frac{\Gamma - 1 + \alpha}{\alpha}\right]\right\} \quad \alpha \neq 1 \tag{6a}$$

$$k_1t = \left(-\frac{1}{\beta}\right)\left[(\beta - 1)\ln\Gamma - \frac{1}{\Gamma} + 1\right] \quad \alpha = 1 \tag{6b}$$

These equations reduce to

$$\Gamma = 1 - \alpha k_1t \tag{7}$$

for short times, a result which of course can also be obtained directly from eq 3. Thus the initial rate yields the photochemical rate constant k_1, and the long-time behavior gives the ratio β.

For order of magnitude estimates, it is known that k_{-1} for other alkylcobalt complexes[8-10] is 10^8–10^9 L/mol·s, and k_2 can similarly be estimated[11] to be 10^7–10^9 L/mol·s. The measured value of k_1 for the light intensity used here is listed in Table I. It can thus be seen from eq 4 that the conditions for the validity of eq 6 are satisfied.

Equation 6 is plotted in Figures 4 and 5 for various values of α and β to display its general behavior and its dependence on these parameters. Particularly noteworthy is the high sensitivity to changes in β. In Figures 6 and 7 the time required to reach a specific value of Γ (fraction of nitroxide remaining) is plotted vs. β (for fixed α). The accurate measurement of β, which is of interest for biophysical studies, can thus be accomplished over several orders of magnitude. Although in principle only one value of Γ (at known time) serves to fix β, greater accuracy is obviously obtained by a least-squares fit of eq 6 to a series of points; this was done in the present work (except that the fit is by eye rather than by least squares). An additional advantage of this procedure is that deviations from eq 6, due to side reactions which might arise unexpectedly in a biochemical system, will become apparent.

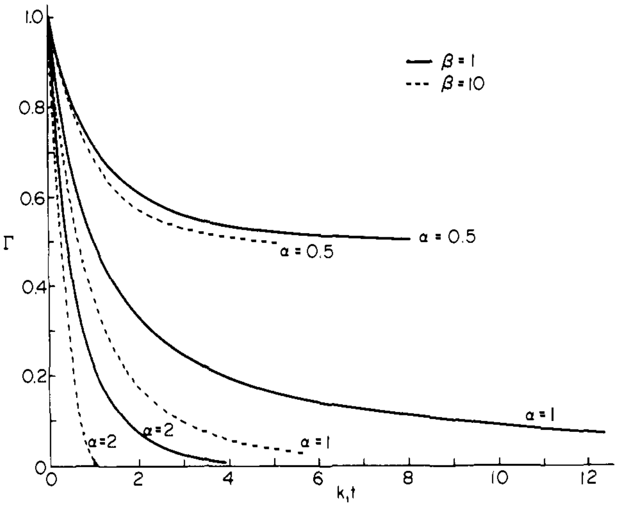

Figure 4. Plots of relative EPR intensity Γ obtained from eq 6 vs. the product of k_1 and time for various values of the parameters α and β (see text).

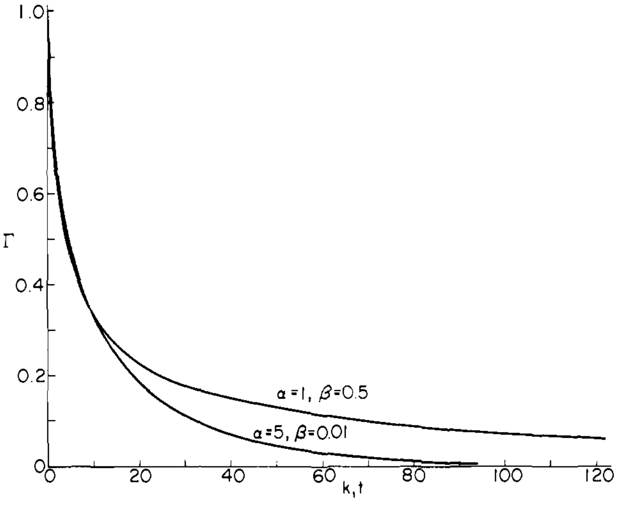

Figure 5. Plot of relative EPR intensity Γ obtained from eq 6 vs. the product of k_1 and time for various values of the parameters α and β, and for long times (see text).

In Figures 1-3 and 8-10 the solid curves drawn are calculated from eq 6, using the value of k_1 obtained from the initial slope (see Table I), and β was adjusted to give a good ("eyeball") fit. In all cases eq 6 is consistent with the data to within experimental error, and predicts all of the unusual features mentioned previously (see "Experimental Observations"). The uncertainty in β is about ±30% for Figures 1-3 and ±40% for Figures 8-10; altering β outside these limits gives curves which are well outside the error limits of the data. The possible discrepancy toward the end of the reaction in Figure 3 is probably due to the neglect of alkyl radical dimerization: using eq 4 one calculates that if $k_{-1} \sim 10^8$, then $B \sim 4 \times 10^{-6}$ M, and when $\Gamma = 0.1$ (and hence $A \simeq 1 \times 10^{-5}$ M), B is no longer negligible with respect to A.

The intrusion of alkyl radical dimerization for initial concentrations lower than $\sim 10^{-5}$ M or power densities higher than $\sim 10^{-4}$ einsteins/cm^2·s is also indicated by a departure from the stoichiometry of eq 1: less alkyl nitroxide is produced, although optical spectra show that the alkylcobalt complex has been destroyed. (Alkyl radical dimerization can be included in the kinetic scheme, but the resulting equations are no longer analytically integrable.)

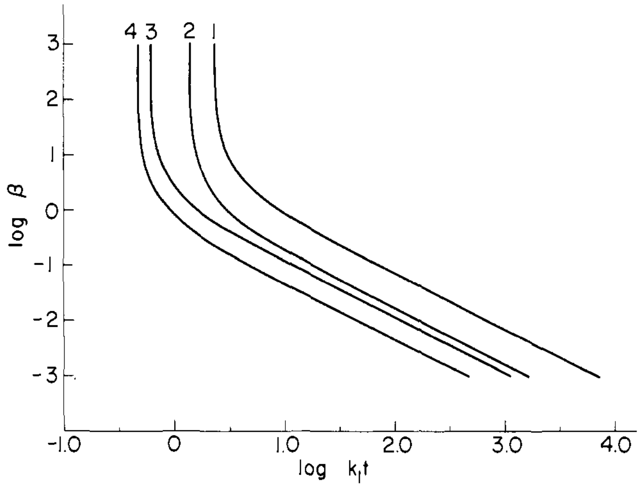

Figure 6. The time required to reach a given Γ (fractional reduction of paramagnetic resonance signal intensity) as a function of the kinetic ratio parameter β for various values of α (see text). (1) $\Gamma = 0.1$, $\alpha = 1$; (2) $\Gamma = 0.25$, $\alpha = 1$; (3) $\Gamma = 0.1$, $\alpha = 2$; (4) $\Gamma = 0.25$, $\alpha = 2$.

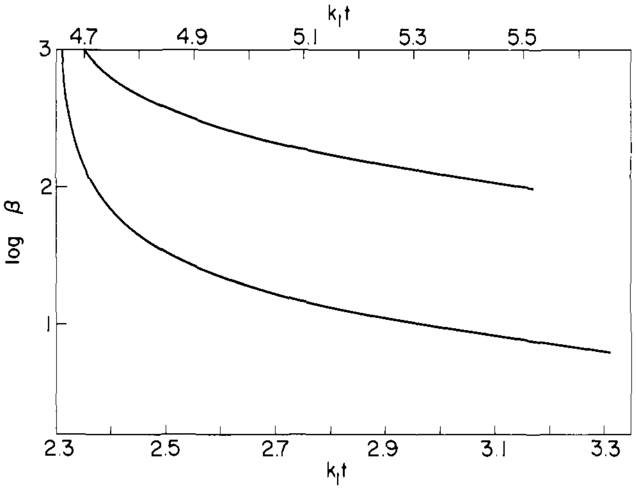

Figure 7. The time required to reach a specified Γ as a function of β (for $\alpha = 1$). Upper curve (upper scale): $\Gamma = 0.01$. Lower curve (lower scale): $\Gamma = 0.1$.

Accurate quantum yields have not been evaluated inasmuch as we have not done any actinometry; however, using the power given by the laser power meter (accuracy not better than 10%) approximate values can be calculated, and these are also given in Table I. They are of the order of magnitude expected from comparison to the results of others[8-10] on macrocyclic tetraamine complexes, indicating that the mechanism of photohomolysis for the alkylpentacyanocobaltates is probably similar to the others. The relative quantum yields calculated can be rationalized on the basis of the influence of charge on the cage recombination probability (although differences arising from electronic structure have certainly not been ruled out).

Phospholipid Multilayer Experiments. Figures 8-10 show the result for the photolysis of coplanar phosphatidylcholine multilayer samples containing 0.2 mol % spin label I and either alkylcobalt complex. The radical functionalities involved are essentially identical with those discussed in the preceding

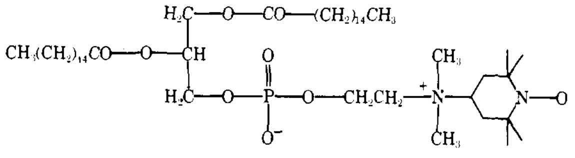

I

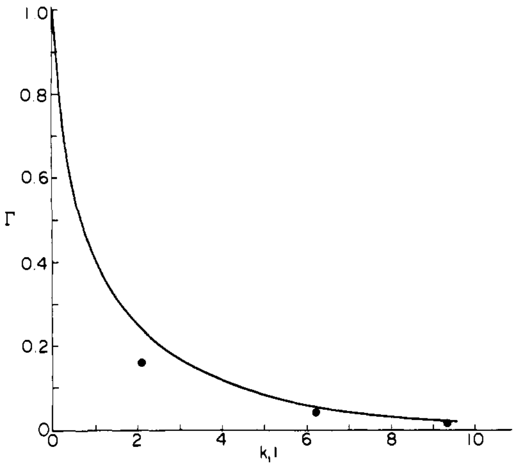

Figure 8. Relative EPR signal intensity Γ vs. the product of k_1 and time for the photolysis of 0.2 mol % spin label I and 0.6 mol % $Co(CN)_5{}^{3-}CH_2CO_2{}^-$ in dimyristoylphosphatidylcholine multilayers, 20.5 °C. Solid line calculated for $\alpha = 3$, $\beta = 0.15$. Laser power 117 mW/cm^2; $k_1 = 0.034$ (note that k_1 in this figure is the product of k_1 from Table I and the ratio of power densities). Uncertainty in Γ is ±0.08, and in β ±40%; these also apply to Figures 9 and 10. (Uncertainty in t is negligible on this scale.)

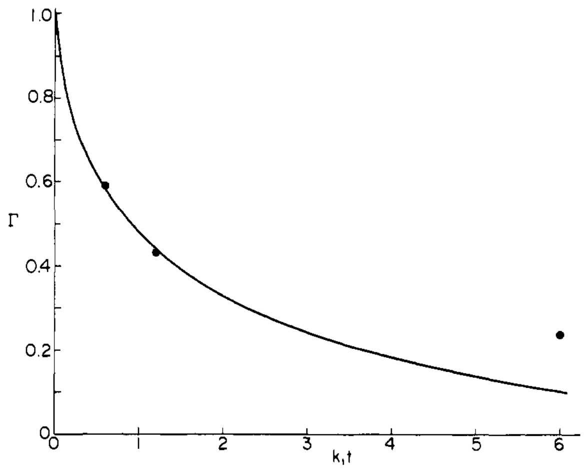

Figure 10. 0.2 mol % spin label I in dimyristoylphosphatidylcholine multilayers with $Co(CN)_5{}^{3-}$ (*N*-methyl)pyridylmethyl; $\alpha = 3$. Solid line calculated for $\beta = 0.1$. $P = 78$ mW/cm^2, $k_1 = 0.04$, $T = 20$ °C.

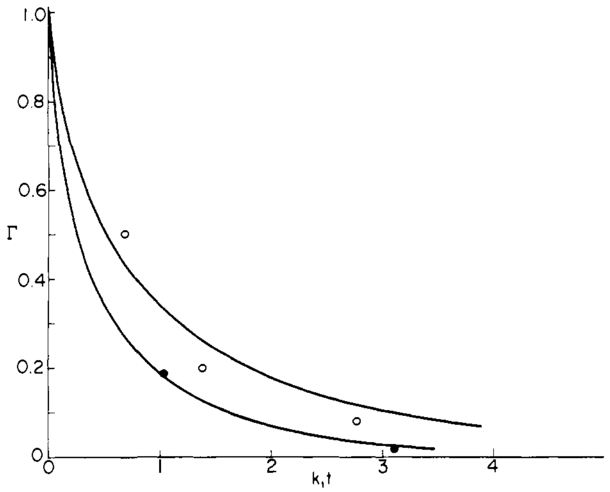

Figure 9. Plots similar to those in Figure 8 except with (closed circles) $\alpha = 7$ (0.2 mol % spin label). Solid line calculated for $\beta = 0.15$. (Open circles) 0.6 mol % spin label I in dipalmitoylphosphatidylcholine multilayers, $\alpha = 2.5$, 48 °C, $P = 157$ mW/cm^2; $k_1 = 0.046$. Solid line calculated for $\beta = 0.3$.

section on bulk solution experiments, yet the value of β is dramatically lower. Since there is no reason to expect k_{-1} to be substantially different, the change must be in k_2, and must reflect a large degree of protection of the membrane-bound nitroxide, even though it is known (for example, by availability of the nitroxide hapten to water-soluble specific antibodies[12]) to be located near or in the aqueous region. There also appears to be a significant difference in β between dimyristoylphosphatidylcholine (below its chain melting transition temperature of 23.5 °C) and dipalmitoylphosphatidylcholine (above its chain melting transition temperature of 41.5 °C).

An even more striking result is obtained when 33 mol % cholesterol is incorporated into the multilayers: β now returns to approximately its bulk solution value. (The binding of specific antibodies against the nitroxide group also increases with increasing cholesterol concentration[12].) There is consequently a very high degree of sensitivity of the rate constant k_2 to bilayer structure. The magnitude of the change shown by these experiments is sufficiently large to suggest that even relatively small structural changes may be detectable by changes in these reaction rates.

In these experiments it is important that there is no reaction of the alkyl radical with components of the membrane other than the nitroxide. For values of $\alpha \leq 10$ no evidence of such reaction has been observed, either by EPR or by thin layer chromatography of the phospholipids.[4,7] In the case of the pyridylmethyl complex, even 100-fold excesses lead to no nonspecific reactions.[5] In addition, even when the nitroxide is attached to the hydrocarbon chains in the bilayer interior, specific reaction with the nitroxide is obtained with the pyridylmethyl complex (unpublished experiments).

Discussion

We anticipate that there may be a number of applications of the foregoing kinetic analysis to problems in membrane biophysical chemistry. One area where this technique should be useful is in cell surface immunology. Previous work[12] has already indicated that the specific conformation of membrane-bound nitroxide haptens can significantly affect both the extent of antibody binding and the degree of complement depletion.[12] The degree of complement depletion has been shown to depend on the degree of activation of the first component of complement (CI).[13] This complement component is activated by its binding to antibodies specifically bound to membrane-bound nitroxide groups. Cellular activation of components of the immune system (e.g., neutrophils) can also be brought about by the specific binding of antibodies to membrane-bound nitroxide groups.[14] Specific antibody dependent activation of these components of the immune system depends strongly on the physical state of the membrane lipids (i.e., whether they are in a "fluid" or "crystalline" state), on the cholesterol content of the bilayer membrane, and on the length of the molecular chain connecting the phosphodiester group and the quaternary nitrogen atom, i.e., $-CH_2CH_2-$ in I. The immunochemical data, as well as the paramagnetic resonance spectra of the nitroxide group itself, suggest that motional freedom and/or structural availability of the nitroxide group to these components of the immune system may play a critical role in their activation. However, other membrane properties, i.e., the rate of lateral diffusion of membrane components, may also be important. The sensitivity of the kinetic parameter β to lipid composition described above strongly suggests that a systematic comparison of these parameters with the rates of immunochemical activation may prove to be a highly useful study, since this kinetic parameter must surely be an index of the availability of the nitroxide group to the aqueous environment surrounding the membrane.

A limitation in the above kinetic analysis is that the quasi-two-dimensional nature of the reaction in multilayer samples has not been taken into account. There are two ways in which this circumstance may manifest itself.

(1) The spin label, which has a diffusion coefficient $\sim 10^{-7}$-10^{-8} cm^2/s in the fluid phase,[4] is essentially "immobile" with respect to the alkyl radicals. Thus a "diffusion-controlled" rate constant may be lowered by a factor of 2 compared to the case where both molecules are equally mobile.

(2) The spin label is constrained to move strictly in the plane of the membrane head-group region, and the free water-soluble molecules are constrained to move in a strip which is only ~20 Å wide, hence nearly but not strictly two-dimensional. The collision probability per unit time, and hence the rate constant, is then enhanced over the three-dimensional case.[15-18] It is difficult to predict the magnitude of this effect precisely but it is not likely to be more than a factor of the order of 4.[18]

Considering the magnitudes of these effects, and the fact that they work in opposite directions, we conclude that the order of magnitude variations we have observed cannot be due to such effects. In more detailed studies they should be considered quantitatively. Non-membrane-bound, water-soluble spin labels can be readily included in multilayer preparations, so that the kinetics with such species can be compared to the membrane-bound case. It is interesting to note that this affords a system for the study of two-dimensional reaction kinetics.[15-18]

There are other useful properties of this reaction which are not dealt with here experimentally, but which the kinetic analysis makes explicit. The fact that the homolysis is reversible in a step of rate comparable to the "forward" irreversible step (k_2) is of the utmost importance, since it allows one to control the lifetime of the alkyl radicals by varying the concentration of Co(CN)$_5^{3-}$.[19] This feature makes the reaction suitable for time-resolved studies of fast processes by flash photolysis.

References and Notes

(1) This work has been supported by the National Science Foundation (Grant PCM 77-23586).

(2) J.R.S. was supported by a National Science Foundation predoctoral fellowship. Department of Chemistry, Massachusetts Institute of Technology, Cambridge, Mass. 02139.

(3) Sheats, J. R.; McConnell, H. M. *J. Am. Chem. Soc.* **1977**, *99*, 7091-7092.

(4) Sheats, J. R.; McConnell, H. M. *Proc. Natl. Acad. Sci. U.S.A.* **1978**, *75*, 4661-4663.

(5) Schwartz, M. A.; McConnell, H. M. *Biochemistry* **1978**, *17*, 837-840.

(6) Berliner, L. G., Ed. "Spin Labeling, Theory and Applications", Academic Press: New York, 1976.

(7) Sheats, J. R. Ph.D. Dissertation, Stanford University, 1978.

(8) Endicott, J. F.; Ferraudi, G. F. *J. Am. Chem. Soc.* **1977**, *99*, 243-245.

(9) Mok, C. Y.; Endicott, J. F. *J. Am. Chem. Soc.* **1977**, *99*, 1276-1277.

(10) Mok, C. Y.; Endicott, J. F. *J. Am. Chem. Soc.* **1978**, *100*, 123-129.

(11) Brownlie, J. T.; Ingold, K. *Can. J. Chem.* **1967**, *45*, 2427-2432.

(12) Brûlet, P; McConnell, H. M. *Biochemistry* **1977**, *16*, 1209-1217.

(13) Esser, A. F.; Bartholomew, R. M.; Parce, J. W.; McConnell, H. M. *J. Biol. Chem.*, in press.

(14) Hafeman, D. G.; Parce, J. W.; McConnell, H. M. *Biochem. Biophys. Res. Commun.*, **1979**, *86*, 522-528.

(15) Naqvi, K. R. *Chem. Phys. Lett.* **1974**, *28*, 280-284.

(16) Deutsch, J. M. *J. Chem. Phys.* **1972**, *56*, 6076-6081.

(17) Suna, A. *Phys. Rev. B* **1970**, *1*, 1716-1739.

(18) Saffman, P. G.; Delbrück, M. *Proc. Natl. Acad. Sci. U.S.A.* **1975**, *72*, 3111-3113.

(19) It was erroneously reported in ref 3 that the Co(CN)$_5^{3-}$ decomposed rapidly. In keeping with other experience,[20] we have found that at concentrations $\leq 10^{-2}$ M it is stable over periods of many hours.

(20) King, N. K.; Winfield, M. E. *J. Am. Chem. Soc.* **1961**, *83*, 3266-3373.

Products and Transients in the Photolysis of Methylated 2-Indanones. Observation and Kinetics of *o*-Xylylenes

K. Kamal de Fonseka, John J. McCullough,* and A. John Yarwood

Contribution from the Department of Chemistry, McMaster University,
Hamilton, Ontario, Canada L8S 4M1.

Received July 3, 1978

Abstract: Transients assigned as *o*-xylylenes have been observed in the flash photolysis of a series of methylated 2-indanones. Thus, 1,1,3,3-tetramethyl-2-indanone gives a transient, assigned as 7,7,8,8-tetramethyl-*o*-xylylene (absorption maximum at 350 nm), while 1,1-dimethyl-2-indanone gives a transient with absorption maximum at 360 nm, assigned as 7,7-dimethyl-*o*-xylylene. Both these transients decay (thermally and photochemically) by a 1,5-hydrogen shift to yield alkyl isopropenylbenzenes. The rates of thermal decay are 0.0020 and 0.038 s^{-1} for the tetra- and dimethyl compounds, respectively, at ca. 20 °C in deoxygenated hexane. The decay of tetramethyl-*o*-xylylene showed a kinetic isotope effect (k_H/k_D) of 5.4. Activation parameters were $E_a = 19$ kcal/mol, $\Delta S^{\circ\ddagger} = -7.7$ eu (tetramethyl-*o*-xylylene); $E_a = 15.5$ kcal/mol, $\Delta S^{\circ\ddagger} = -13.9$ eu (dimethyl-*o*-xylylene). Photolysis of 1,1,3,3-tetramethyl-4,5-benzindan-2-one gives the thermally stable 9,9,10,10-tetramethyl-1,2-naphthoquinodimethane, which decays photochemically to 1-isopropenyl-2-isopropylnaphthalene. A transient with a lifetime of about 5 μs could be observed in the flash photolysis of 1,1,3,3-tetramethyl-5,6-benzindan-2-one, which gives two photoproducts: 2-isopropyl-3-isopropenylnaphthalene and 3,3,4,4-tetramethylnaphtho[*b*]cyclobutene. The rates of thermal decay of the transients are consistent with thermochemical calculations. Spectroscopic evidence, together with theoretical calculations, indicates that the transients are twisted about the "essential" single bonds of the nonaromatic ring, and cannot adopt the planar geometry necessary for the allowed suprafacial 1,5-H shift. This, together with the photolability of the transients, suggests that the thermal decay may involve the previously unknown antarafacial 1,5-hydrogen shift.

We have previously shown that the *o*-quinonoid species isoindenes can be generated by aryl migration on photolysis of 1,1-diarylindenes.[1] In the former study, we used kinetic isotope effects, substituent effects, and activation parameters to characterize the decay pathway of the isoindene transients. It was concluded that the data were consistent with a suprafacial 1,5-hydrogen shift (giving stable indenes) as the mode of decay. *o*-Quinonoid species have been produced by photolysis of various 2-indanones.[2] In a paper in 1966, Starr and Eastman[3] studied the photodecarbonylation of 1,1,3,3-tetra-

0002-7863/79/1501-3277$01.00/0